AIAA 91-0690
Effects of Ambient Gas Density on the Structure of Pressure-Atomized Sprays

L.-K. Tseng, G. A. Ruff and G. M. Faeth
The University of Michigan
Ann Arbor, MI

29th Aerospace Sciences Meeting
January 7-10, 1991/Reno, Nevada

AIAA-91-0690

EFFECTS OF AMBIENT GAS DENSITY ON THE STRUCTURE OF PRESSURE-ATOMIZED SPRAYS

L.-K. Tseng,* G. A. Ruff† and G. M. Faeth‡
The University of Michigan
Ann Arbor, Michigan 48109-2140

Abstract

A theoretical and experimental study of the dense-spray region of pressure-atomized nonevaporating sprays is described, emphasizing effects of ambient gas density in the atomization breakup regime. Mean liquid volume fraction distributions were measured for 9.5 mm diameter water jets in still air at pressures of 1-8 atm. Mixing was strongly affected by the gas/liquid density ratio and the degree of flow development at the jet exit, with the largest gas/liquid density ratio and fully-developed turbulent pipe flow yielding the fastest mixing rates. Predictions based on the locally homogeneous flow approximation, where relative velocities between the phases are assumed to be small in comparison to mean flow velocities, were in good agreement with measurements, including representation of effects of gas/liquid density ratio and flow development at the jet exit.

Nomenclature

d	= injector exit diameter
d_p	= drop diameter
f	= mixture fraction
k	= turbulence kinetic energy
L	= injector passage length
Oh	= Ohnesorge number, $\mu_f/(\rho_f d\sigma)^{1/2}$
p	= pressure
r	= radial distance
Re_f	= jet Reynolds number, $\rho_f d u_o/\mu_f$
u	= streamwise velocity
v	= radial velocity
w	= tangential velocity
We_{id}	= Weber number based on phase i and the jet diameter, $\rho_i d u_o^2/\sigma$
We_{gp}	= drop Weber number, $\rho_g d_p u_o^2/\sigma$
x	= streamwise distance
α	= volume fraction
ϵ	= rate of dissipation of turbulence kinetic energy
μ	= molecular viscosity
ρ	= density
σ	= surface tension
ϕ	= generic property

Subscripts

c	= centerline value
f	= liquid-phase property
g	= gas-phase property
o	= injector exit conditions
∞	= ambient conditions

Superscripts

$\bar{(\ )}(,\bar{(\ )}')$	= time-averaged mean and rms fluctuating quantities
$\tilde{(\ )}(,\tilde{(\ )}")$	= Favre-averaged mean and rms fluctuating quantities

Introduction

An experimental and theoretical investigation of the near-injector, dense-spray, region of nonevaporating round pressure-atomized sprays is described. This flow is of interest for a variety of atomization and gas/liquid mixing processes; it also merits study as the multiphase counterpart of the single-phase turbulent jet. The objective of the research was to extend earlier studies of round water jets in still room air,[1-3] to consider effects of ambient gas density on the structure and mixing properties of the flow. Measurements of liquid volume fraction distributions were completed in the near injector region of water jets in still air at various ambient pressures. Tests were limited to the atomization breakup regime, where liquid breakup into drops and the development of a multiphase mixing layer begins right at the jet exit, since this regime is most important for practical applications.[4,5] Jet exit conditions included both fully-developed turbulent pipe flow and low-turbulence intensity slug flow due to the known importance of the degree of flow development at the jet exit on dense spray properties.[1-3,6] The measurements were used to evaluate predictions of effects of gas/liquid density ratio on flow properties, found from an earlier model based on the locally-homogeneous flow (LHF) approximation,[1] i.e., the assumption that relative velocities between the phases are small in comparison to mean flow velocities.

Only the main features of past work will be considered, since reviews treating dense sprays have appeared recently.[7,8] Earlier measurements have established the main features of the near injector region of pressure-atomized sprays within the atomization breakup regime. The flow consists of a liquid core, much like the potential core of a single-phase jet, surrounded by a dispersed drop/gas mixing layer. Conductivity probes have been used to study the length of the liquid core at various ambient gas densities.[6,9,10] The liquid core tends to become shorter at high ambient gas densities due to increased entrainment rates. Nevertheless, the liquid core and its multiphase mixing layer are prominent features of pressure-atomized sprays for typical gas/liquid density ratios, extending 200-400 injector diameters from the jet exit for liquid injection into gases at atmospheric pressure.[9]

Recent measurements of Ruff et al.[1-3] have yielded some information about the structure of the dense-spray region of

* Graduate Assistant, Department of Aerospace Engineering.
† Graduate Assistant, Department of Aerospace Engineering; currently Assistant Professor, Department of Mechanical Engineering, Drexel University, Philadelphia, Pennsylvania.
‡ Professor, Fellow AIAA.

pressure-atomized sprays. These experiments involved large (9.5 and 19.1 mm initial diameters) water jets injected into still air at atmospheric pressure. Measurements included liquid volume fraction distributions using gamma-ray absorption, drop sizes and velocities in the mixing layer using double-pulse holography, and air entrainment rates using laser velocimetry. The measurements of mean liquid volume fraction distributions showed that the rate of development of the flow was affected by both the breakup regime and the degree of flow-development at the jet exit: atomization breakup and fully-developed turbulent pipe flow at the jet exit yielded the fastest mixing rates. Predictions based on the LHF approximation were effective for atomization breakup when mean liquid volume fractions were greater than 0.2; however, they progressively failed as the flow became dilute and as jet exit conditions approached the wind-induced breakup regime. Difficulties with the LHF approach were identified by drop size and velocity measurements in the mixing layer, which indicated significant effects of separated flow in regions where liquid volume fractions were low. Thus, the success of the LHF approximation at large liquid volume fractions was attributed to the small proportion of the momentum associated with the gas phase at these conditions due to the small gas/liquid density ratio of the flow. Similarly, entrainment rates are governed mainly by processes within the dilute portions of the mixing layer; therefore, LHF predictions generally overestimated entrainment rates due to separated-flow phenomena in the mixing layer. However, the findings suggested improved performance of LHF methods at large We_f, with this limit approached more rapidly at large gas/liquid density ratios.

The objective of the present investigation was to explore effects of gas/liquid density ratio on the mixing properties of pressure-atomized sprays and the adequacy of predictions based on the LHF approximation. Experiments involved visualization of the flow and measurements of liquid volume fraction distributions within large-scale (9.5 mm initial jet diameter) water jets in still air at pressures of 1-8 atm. The measurements were compared with predictions based on the earlier LHF approach,[1,2] to determine whether this methodology could treat effects of varying gas/liquid density ratios.

The paper begins with brief descriptions of experimental methods and the LHF computations. Results are then described, considering flow visualization and liquid volume fraction distributions in turn.

Experimental Methods

Apparatus

Experimental methods were similar to Ruff et al.[1], except that the flow was contained within a large pressure vessel so that the pressure of the ambient air could be changed. A sketch of the apparatus appears in Fig. 1. The arrangement involves a steady water jet injected vertically downward in still air within a large windowed pressure vessel (1.5 m diameter × 4.5 m long with two pairs of opposite windows having maximum opening diameters of 250 mm). Access to the interior of the pressure vessel, for assembly and adjustment of the jet apparatus, was provided by a manhole at the top of the vessel. A second port at the top provided entry points for water to the jet and electrical cables needed for the jet traversing system.

City water was fed to the injector using a centrifugal pump. The water was collected in the bottom of the tank with the liquid level maintained by outflow to a drain. A grate located above the liquid level reduced splashing back into the test area. The rate of water flow was adjusted using a bypass system and was measured using a turbine flow meter that was calibrated by collecting water for timed intervals.

The water injectors had exit diameters of 9.5 mm and were the same as those used by Ruff et al.[1]: one yielding slug flow with low turbulence intensities, the other yielding fully-developed turbulent pipe flow. The slug flow injector consisted of a honeycomb flow straightener (1.6 mm cells, 25 mm long) and two screens to calm the flow (16 × 16 square mesh, 0.18 mm diameter wire) followed by a 13.6:1 area contraction to the jet exit. The fully-developed flow injector had the same flow straightener and contraction area ratio but the contraction was followed by a constant area passage 41 injector diameters long.

Instrumentation was mounted rigidly so that flow structure was measured by traversing the injector. Horizontal traverses were carried out using a stepping motor driven linear positioner with a positioning accuracy of 5 μm. Vertical traverses involved moving the injector assembly along linear bearings with a manual positioner having a positioning accuracy of 0.5 mm.

Instrumentation

Flow Visualization. Flash photography was used to study the appearance of the flow. The light source was a Xenon Corp. high-intensity micropulse system (model 457A) which generates up to a 10J light pulse having a 1 μs duration. The photographs were obtained in a darkened room, directing the light source and camera through adjacent windows on one side of the apparatus. A 4 × 5 Speed Graphic Camera loaded with Polaroid type 57 black and white film (ASA 3000) was used for the photographs. The camera was operated with the lens open, using the flash duration to control the time of exposure. The field of view of the spray on the photographs was roughly 200 mm long.

Gamma-Ray Absorption. Distributions of mean liquid volume fractions were measured using gamma-ray absorption similar to Ruff et al.[1] An Iodine-125 isotope source (5 mCi, emitting primarily at 27.20, 27.47 and 31.00 keV) provided a soft gamma-ray source with good absorption levels. The source was placed in a lead casket with an outlet aperture 1.6 mm in diameter and 13 mm long. Gamma rays passing through the flow were detected and counted with a Bicron X-ray probe (Model 1 × M.040/1.54) and a EG&G Ortec single-channel analyzer and counter/timer (models 556, 590A, 974). A lead aperture (1.5 mm in diameter and 12 mm long) was placed in front of the detector to define the path observed through the flow. The energy window of the detector was set at 22-32 keV to minimize spurious counts due to background radiation and Compton scattering. The source and detector were placed in recessed mounts within opposing windows of the apparatus (not shown in Fig. 1) so that they were separated by a distance of 500 mm with the radiation path crossing horizontally through the chamber axis.

Absorption measurements (based on 20000-25000 counts) were made for 30-60 parallel paths through the flow and

deconvoluted in the same manner as Santoro et al.[12] and Ruff et al.[1] The narrow absorption path minimized potential errors due to the orientation of liquid elements to less than 5%.[13] Experimental uncertainties were largely due to finite sampling times and background from the small drops dispersed within the pressure vessel. They are estimated (95% confidence) to be less than 30% for $\bar{\alpha}_f > 0.01$.

Test Conditions

Test conditions are summarized in Table 1. Operating conditions were selected to yield the same mean jet exit velocity for fully-developed and slug flow at pressures of 1, 2, 4 and 8 atm. within the atomization breakup regime. Due to the limitations of the pump, this required a water flowrate roughly 13% lower than the atomization breakup condition used by Ruff et al.[1-3] for the 9.5 mm diameter injector. However, all test conditions are well into the atomization breakup regimes defined by Ranz[4] and Miesse,[5] and exhibited initial liquid breakup right at the jet exit which is characteristic of this breakup regime.

Flow properties at the exit of the injector were measured earlier using laser velocimetry.[1] For fully-developed flow, mean streamwise velocity distributions were in good agreement with values in the literature for the same Reynolds number range.[14] However, rms streamwise and radial velocity fluctuations were more uniform across the central region, yielding streamwise and radial turbulence intensities of 7 and 4% near the axis, which are somewhat larger than literature values.[14] For slug flow, mean streamwise velocities were uniform over the central region of the flow and then declined near the wall (within 3-5% of the injector radius) due to boundary layer growth in the nozzle passage. Streamwise and radial rms velocity fluctuations were roughly 1% of the mean streamwise velocity over the central region for slug flow.[1]

Theoretical Methods

Predictions of flow properties were limited to use of the LHF approximation similar to past work.[1,2,7] In addition to the LHF approximation, the major assumptions of the model are as follows: steady (in the mean) axisymmetric flow with no swirl, boundary layer approximations apply, negligible kinetic energy and viscous dissipation of the mean flow, buoyancy only affects the mean flow, equal exchange coefficients of all species and phases, and negligible mass transport between the phases (evaporation). These assumptions are either conditions of the experiments or are justified by past practice, except for the LHF approximation which will be evaluated by the measurements. In particular, operation of well-atomized sprays within a closed container saturated the air with water vapor so that there was no potential for liquid evaporation.

Under these assumptions, the instantaneous mixture fraction is either 0 (in the gas) or 1 (in the liquid). Then, time- and Favre-averages of any scalar property, ϕ, can be found in terms of the Favre-averaged mean mixture fraction, as follows:

$$\tilde{\phi} = \phi_\infty(1 - \tilde{f}) + \phi_0\tilde{f} \qquad (1)$$

$$\bar{\phi} = (\phi_\infty\rho_0(1- \tilde{f}) + \phi_0\rho_\infty\tilde{f}) / (\rho_0(1 - \tilde{f}) + \rho_\infty\tilde{f}) \qquad (2)$$

Given Eqs. (1) and (2), the flow field can be found from a simplified version of the conserved-scalar formalism of Lockwood and Naguib,[15] but using Favre averages following Bilger.[16] Governing equations are solved for conservation of mass, streamwise mean momentum, mean mixture fraction, turbulence kinetic energy and the rate of dissipation of turbulence kinetic energy. The specific formulation, all empirical constants, and a discussion of calibration of the approach for a variety of constant and variable density single-phase jets, appears elsewhere.[7]

The specification of initial and boundary conditions, and the details of the numerical computations, can be found in Ruff et al.[1,2] For fully-developed flow, initial profiles of $\tilde{u}$, k and ε were taken from Schlichting[14] and Hinze.[17] For slug flow, properties were assumed to be uniform except for bounding estimates of properties in the boundary layer along the wall for L/d = 0 and 5, with the latter conditions found assuming clean entry and no *vena contracta* along the nozzle passage from Schlichting.[14]

Results and Discussion

Flow Visualization

Flash photographs of the near-injector region, up to 200 mm from the jet exit, are illustrated in Fig. 2 for fully-developed flow and Fig. 3 for slug flow. In each case, results are shown for ambient pressures of 1, 2, 4 and 8 atm. The photographs for both jet exit conditions exhibit a progressively increasing flow width with increasing ambient density in addition to the usual increase of flow width with increasing distance from the injector due to mixing. This suggests faster mixing or entrainment rates as the gas/liquid density ratio increases. Such behavior is analogous to single-phase variable density jets which generally have faster mixing and entrainment rates as the ratio of ambient/injected density increases.[18]

A second feature of the flash photographs of Figs. 2 and 3 is that the jets become less coarse and have a more wispy appearance as the pressure increases. This suggests smaller drop sizes within the bulk of the multiphase mixing layer, which is expected based on consideration of maximum drop sizes after secondary breakup. For example, Ruff et al.[2,3] find that the largest drops, excluding the near surface region where drops have only undergone primary breakup, have velocities comparable to the jet exit velocity and sizes comparable to the limiting criterion for secondary breakup, $We_{pg} = \rho_g d_p u_0^2/\sigma \approx 6.5$ discussed by Clift et al.[19] This implies that maximum drop sizes after secondary breakup are related to jet exit conditions as follows: $d_p/d \approx 6.5/We_{gd}$. For present test conditions, We_{gd} increases from 380 to 3020 as the ambient pressure increases from 1-8 atm., so that d_p/d after secondary breakup should decrease nearly an order of magnitude as the pressure changes in this range. This supports the existence of larger numbers of smaller drops near the edge of the flow at high pressures, yielding the more wispy appearance at high pressures seen in Figs. 2 and 3.

A third feature of the flash photographs of Figs. 2 and 3 is the striking difference between fully-developed and slug flow jet exit conditions: the fully-developed flows are significantly wider at each gas pressure, indicating faster mixing rates. Similar behavior with respect to increased turbulence levels at the jet exit has been observed by Phinney[6] and Ruff et al.,[12] among others. Such behavior is expected due to the well known

enhancement of mixing of single phase jets with increased turbulence levels at the jet exit, at least to the extent that LHF ideas are appropriate.[7] For the present flows, liquid-phase turbulence is particularly important because the momentum of the liquid dominates flow properties due to the large liquid/gas density ratio. Viewed from the perspective of separated flow effects, Ruff et al.[2,3] find that drop sizes after primary breakup near the liquid surface are much larger for fully-developed turbulent flow than for slug flow. These larger drops maintain radial velocities present at the time of primary breakup, due to their inertia and slow rates of secondary breakup, causing them to penetrate more effectively in the radial direction. This causes mixing rates to increase with increased turbulence levels at the jet exit, even though drop sizes after primary breakup increase as well.

Mean Liquid Volume Fractions

The mean liquid volume fraction distributions provide a quantitative indication of effects of gas/liquid density ratio and jet exit conditions on flow properties. However, it is important to recognize the relationship between liquid volume fractions and mixing levels when interpreting these results. Present flows have large liquid/gas density ratios which implies that liquid volume fractions vary rapidly with mixture fraction. This can be seen from the state relationship for liquid volume fraction:

$$\alpha_f = f/(f + (\rho_f/\rho_g)(1-f)) \qquad (3)$$

Table 2 is a summary of values of f for α_f =0.1 and 0.01 over the present ambient pressure range. It is evident from the table that low levels of mixing cause large reductions in liquid volume fractions, even at the highest ambient pressures of the present test range. Thus, $\bar{\alpha}_f$ is an unusually sensitive indicator of mixing levels in the near-injector region.

Measured and predicted time-averaged mean liquid volume fractions along the axis are illustrated in Figs. 4 and 5 for fully-developed and slug flow jet exit conditions, respectively. Results are plotted as a function of distance from the injector, normalized by the injector diameter, with ambient pressure as a parameter. Predictions for slug flow jet exit conditions are shown for L/d = 0 and 5, which bounds the potential degrees of flow development within the nozzle passage, as noted earlier. Measurements of Ruff et al.[1] at 1 atm. and atomization breakup are not shown on the plots to reduce clutter; however, they agree very well with present results even though jet exit velocities are slightly different. This behavior is expected based on the LHF predictions, which exhibit very little variation of liquid volume fraction distributions with jet exit velocity for the high Reynolds numbers of present flows.

For fully-developed flow, Fig. 4, the near-injector region (x/d < 3-8) exhibits mean liquid volume fractions near unity. Just beyond this region, however, mean liquid volume fractions decrease rapidly, reaching values on the order of 0.1 for x/d in the range 50-100. The initial reduction of $\bar{\alpha}_{fc}$ occurs at progressively smaller values of x/d as the pressure increases, with values of $\bar{\alpha}_{fc}$ at a given value of x/d generally being lower at higher pressures as well. These trends indicate faster mixing rates at higher ambient gas densities, analogous to effects of flow density ratio for single-phase turbulent jets.[18] There is good agreement between measurements and predictions, indicating that the LHF approach correctly treats effects of the density ratio of the flow on mixing properties. However, present findings illustrated in Fig. 4 also represent relatively low levels of mixing, e.g., results in Table 2 suggest that mixture fractions are generally greater than 0.9. For such low levels of mixing, predictions based on LHF approximation have been reasonably good in the past,[1] because separated flow effects due to relative velocity differences between the gas and liquid are not very significant when the mass of the flow is predominantly liquid. Based on past evaluations of the methodology,[7] performance of the LHF approach is likely to be poorer as the dilute dispersed flow regime, where f << 1, is approached. Finally, even though the variation of $\bar{\alpha}_{fc}$ suggests a relatively short liquid core, this is not the case when viewed in terms of mixture fraction. Mixture fractions are generally greater than 0.9 for the results illustrated in Fig. 4 so that even low levels of flapping of the liquid core can explain the reductions of $\bar{\alpha}_{fc}$.

The slug flow results illustrated in Fig. 5 exhibit slower rates of mixing than the fully-developed flows. First of all, $\bar{\alpha}_{fc}$ remains at unity until x/d is in the range 20-50 so that $\bar{\alpha}_{fc}$ at each x/d is higher for slug than for fully-developed flow. Similar to the results for fully-developed flow, however, the value of x/d where $\bar{\alpha}_{fc}$ first begins to decrease from unity progressively decreases as the pressure increases, implying faster rates of mixing at higher ambient densities. The strong effect of the degree of flow development at the jet exit (compare Figs. 4 and 5) is similar to earlier observations at atmospheric pressure.[1] This comes about because the liquid density is large in comparison to the gas; therefore,the fully-developed flow carries significant levels of turbulence energy into the mixing layer, which enhances mixing rates. Predictions of properties for slug flow conditions are very sensitive to the degree of flow development at the jet exit which implies that even small levels of liquid vorticity at the jet exit can have a significant effect on flow properties. Thus, there are significant differences between predictions for pure slug flow (L/d = 0) and allowance for boundary layer growth within the injector passage (L/d = 5). These conditions bound the range of possibilities for present tests, and it is encouraging that the two predictions tend to bound the measurements except at x/d = 100 and pressures of 4 and 8 atm. The discrepancies at x/d = 100 occur in a region where the streamwise variation of flow properties is rapid, and tends toward dilute conditions. Thus, since both predictions tend to overestimate the rate of development of the flow, separated flow effects are probably responsible for the difficulty. However, small initial levels of liquid vorticity have a very strong effect on flow properties for slug flow; therefore, an influence of injector disturbances can not be ruled out.

Predicted and measured radial profiles of mean liquid volume fractions for fully-developed flow are illustrated in Figs. 6-8 for ambient pressures of 1, 2 and 4 atm. (results atm 8 atm. are similar). These results involve $\bar{\alpha}_f/\bar{\alpha}_{fc}$ plotted as a function of radial distance normalized by the injector radius, so that the actual width of the flow can be seen. Results are shown for various x/d $\leq$ 100 because larger distances risked disturbances of the flow from the chamber walls. The measurements show a progressive increase of flow width with increasing distance from the jet exit, with flow widths increasing at a fast rate at higher pressures. Apparent flow radii based on $\bar{\alpha}_f/\bar{\alpha}_{fc}$, however, are much smaller than for single-phase jets. For example, the edge of the flow at x/d = 100 is at 2r/d = 2.5-3.0, which implies a flow edge at r/x = 0.012-0.015. In comparison, the flow width based on scalar properties in the fully-developed region of turbulent jets is r/x $\approx$

0.15, nearly an order of magnitude larger. Much of this behavior is due to the strong sensitivity of $\bar{\alpha}_f$ to the mixing level, noted in connection with results summarized in Table 2. Notably, flow widths based on mean void fraction distributions for gas jets in liquids are unusually large for similar reasons.[20] For both turbulent liquid jets in gases and gas jets in liquids, however, predictions using the LHF approach indicate relatively normal flow widths far from the jet exit, when they are based on $\tilde{f}$. Unfortunately, direct experimental verification of this behavior

Predicted and measured radial profiles of mean liquid volume fractions for slug flow are illustrated in Figs. 9-11 for ambient pressures of 1, 2 and 4 atm. (results at 8 atm. are similar). Predictions for L/d = 0 and 5 are shown, similar to Fig. 5, in order to bound the potential range of flow development at the jet exit. In this case, there is a relatively sharp transition between the liquid core of the flow and the region where $\bar{\alpha}_f$ decreases, at least for $x/d \leq 50$. Additionally, the extent of radial spread of the slug flows is less than the fully-developed flows, e.g. the flow widths at x/d = 100 are in the range 2r/d = 2.0-2.5 rather than 2.5-3.0 which was the range for fully-developed flow. Both these observations are consistent with slower mixing rates for slug flow than fully-developed flow. Predictions are reasonably good for $x/d \leq 25$, within the bounds of the limiting estimates of the degree of flow development at the jet exit. Farther from the injector, however, predictions are less satisfactory. In particular, errors are large in the region where $\bar{\alpha}_{fc}$ first begins to decrease from unity, see Fig. 5. This behavior is caused by poor estimates of $\bar{\alpha}_{fc}$, due to uncertainties in the initial degree of flow development, since $\bar{\alpha}_{fc}$ is used to normalize both predictions and measurements in Figs. 9-11. Beyond this region, predictions are in better agreement with measurements but this is largely fortuitous because $\bar{\alpha}_{fc}$ is still not predicted very well by either limiting condition (see Fig. 5). These difficulties are probably due to the effects of separated flow in the rapidly developing region near the tip of the liquid core for slug flow, as discussed earlier.

Sensitivity Study

The sensitivity of present computations was examined similar to past work.[1,2] Predictions were very sensitive to initial mean velocity distributions, as can be seen from the results illustrated in Figs. 5 and 9-11 for slug flow at the limits L/d = 0 and 5. Predictions were also sensitive to initial values of k and ε. However, these properties were reasonably well known for the fully-developed flows, while effects of low turbulence levels in the case of the slug flow were not very significant. Thus, the uncertainties of the predictions were largely governed by difficulties in specifying the mean velocity distribution for slug flows, and the less quantifiable limitations of k-ε turbulence models using the LHF approximation for multiphase boundary layer flows.

Conclusions

The near-injector dense-spray region of pressure-atomized sprays was studied for various ambient gas densities at atomization breakup conditions. The major conclusions of the study are as follows:

1) Increasing gas/liquid density ratios reduces the length of the liquid core and increases the flow width, implying increased rates of mixing analogous to effects of density ratio for single-phase turbulent jets.
2) Turbulence levels and the degree of flow development at the jet exit have a strong effect on mixing rates, with turbulent liquids mixing much faster than nonturbulent liquids containing little vorticity.
3) Use of the locally-homogeneous-flow approximation, in conjunction with a Favre-averaged turbulence model, yielded good estimates of effects of gas/liquid density ratio and initial liquid vorticity on time-averaged liquid volume fraction distributions. The main limitations were associated with problems of prescribing jet exit conditions for slug flows, due to the sensitivity of flow properties in low levels of vorticity at the jet exit.

Present conclusions are based on large-scale sprays (9.5 mm injector diameter) that have much lower rates of deceleration than practical injectors, and regions of the flow having relatively high mixture fractions (generally greater than 0.9 along the axis) where the momentum of the gas does not have a strong influence on flow dynamics. These factors favor use of the locally-homogeneous flow approximation, so that present observations are not necessarily in conflict with earlier work showing significant separated-flow effects within dense sprays for smaller injector diameters and mixture fractions.[1-3,7] Additional information concerning liquid breakup properties in dense sprays is clearly needed in order to provide a rational means of evaluating separated-flow effects and the adequacy of the locally-homogeneous-flow approximation for particular conditions.

Acknowledgements

This research was supported by ONR Grant No. N00014-89-J-1199 with G. D. Roy serving as Scientific Officer. Initial development of the variable ambient density test chamber was sponsored by the Air Force Office of Scientific Research, under Grant No. AFOSR-85-0244, with J. N. Tishkoff serving as Program Manager. The U.S. Government is authorized to reproduce and distribute copies of this report for governmental purposes notwithstanding any copyright notation thereon.

References

[1]Ruff, G.A., Sagar, A.D. and Faeth, G.M., "Structure of the Near-Injector Region of Pressure-Atomized Sprays," AIAA J., Vol.27, July 1989, pp. 549-559.

[2]Ruff, G.A., Bernal, L.P. and Faeth, G.M., "Structure of the Near-Injector Region of Non-Evaporating Pressure-Atomized Sprays," J. Prop. Power, 1990, in press.

[3]Ruff, G.A., Bernal, L.P. and Faeth, G.M., "Continuous- and Dispersed-Phase Structure of Dense Nonevaporating Pressure-Atomized Sprays," J. Prop. Power, submitted.

[4]Ranz, W.E., "Some Experiments on Orifice Sprays," Can. J. Chem. Engrg, Vol. 36, Aug. 1958, pp. 175-181.

[5]Miesse, C.C., "Correlation of Experimental Data on the Disintegration of Liquid Jets," Ind. Engr. Chem. Vol. 47, Sep. 1955, pp. 1690-1697.

[6]Phinney, R.E., "The Breakup of a Turbulent Jet in a Gaseous Atmosphere," J. Fluid Mech., Vol. 6, Oct. 1973, pp. 689-701.

[7]Faeth, G.M., "Mixing, Transport and Combustion in Sprays," Prog. Energy Combust. Sci., Vol. 13, 1987, pp. 293-345.

[8]Faeth, G.M., "Structure and Atomization Properties of Dense Turbulent Sprays," Twenty-Third Symposium (International) on Combustion, The Combustion Institute, Pittsburgh, 1990, in press.

[9]Chehroudi, B., Onuma, Y., Chen, S.-H. and Bracco, F. V., "On the Intact Core of Full Cone Sprays," SAE Paper No. 850126, 1985.

[10]Hiroyasu, H., Shimizu, M., and Arai, M., "The Breakup of a High speed Jet in a High Pressure Gaseous Environment," Univ. of Wisconsin, Madison, ICLASS-82, 1982.

[11]Smith, R.H. and Wang, C.-T., "Contracting Cones Giving Uniform Throat Speeds," J. Aero. Sci., Vol .11, October, 1944, pp. 356-360.

[12]Santoro, R.J., Semerjian, J. H., Emmerman, P.J., and Goulard, R., "Optical Tomography for Flow Field Diagnostics," Int. J. Heat Mass Trans., Vol. 24, July 1981, pp. 1139-1150.

[13]Gomi, H. and Hasegawa, K.I., "Measurements of the Liquid Phase Mass in Gas-Liquid Sprays by X-ray Attenuation," Int. J. Multiphase Flow, Vol. 10, Dec. 1984, pp. 653-662.

[14]Schlichting, H., Boundary Layer Theory. McGraw-Hill, New York, 7th ed., 1979, p. 599.

[15]Lockwood, F.C. and Naguib, A.S., "The Prediction of Fluctuations in the Properties of Free, Round-Jet Turbulent Diffusion Flames," Combust. Flame, Vol. 24, Feb. 1975, pp. 109-124.

[16]Bilger, R.W., "Turbulent Jet Diffusion Flames," Prog. Energy Combust. Sci., Vol. 1, 1976, pp. 87-109.

[17]Hinze, J.O., Turbulence, 2nd ed., McGraw-Hill, New York, 1975, p. 427 and pp. 724-734.

[18]Ricou, F.P. and Spalding, D.B., "Measurements of Entrainment by Axisymmetrical Turbulent Jets," J. Fluid Mech., Vol. 11, Jan. 1961, pp. 21-32.

[19]Clift, R., Grace, J.R. and Weber, M.E., Bubbles, Drops and Particles, Academic Press, New York, 1978, p. 346.

[20]Loth, E. and Faeth, G.M., "Structure of Underexpanded Round Air Jets Submerged in Water. Int. J. Multiphase Flow, Vol. 15, Dec. 1989, pp. 589-603.

Table 1 Summary of test conditions[a]

Injector diameter (mm)	9.5
Ambient pressure (atm.)	1, 2, 4 and 8
Jet flow rate (kg/s)	3.47
Injector pressure drop (kPa):	
Fully-developed flow	2270
Slug flow	2110
Average jet exit velocity (m/s)	49.1
Re_f	462,000
We_{fd}	312,000
We_{gd}	380, 760, 1520, 3040
Oh	0.00121

[a]Pressure-atomized water jet injected vertically downward in still air at various pressures and 298 ± 2K; in atomization breakup regime for both slug flow and fully-developed turbulent pipe flow (L/d = 41) jet exit conditions.

Table 2 f vs α_f for air/water mixtures[a]

α_f	Pressure (atm.)			
	1	2	4	8
0.01	0.990	0.979	0.960	0.923
0.01	0.897	0.813	0.684	0.520

[a]Air/water mixtures at 300 K and various pressures.

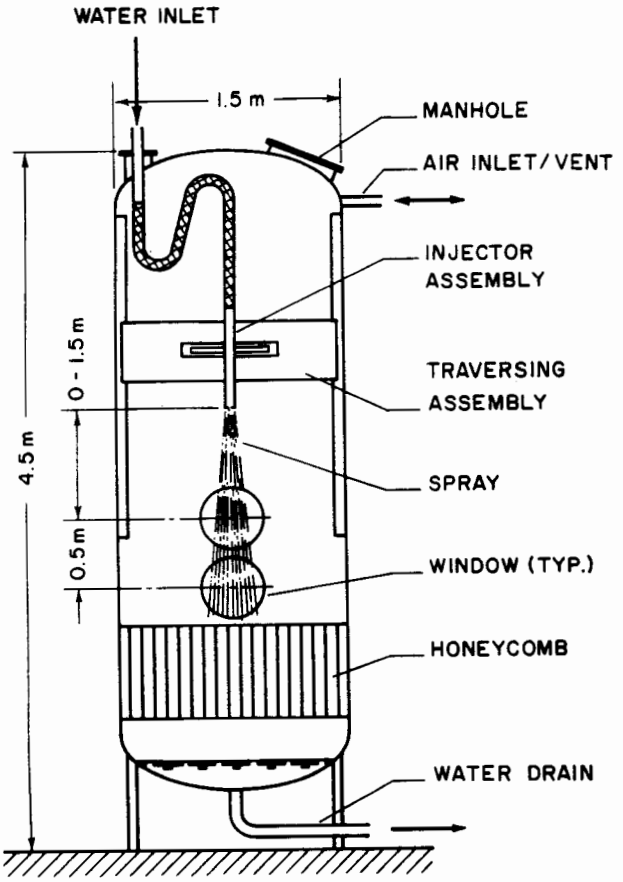

Fig. 1 Sketch of the variable gas density apparatus.

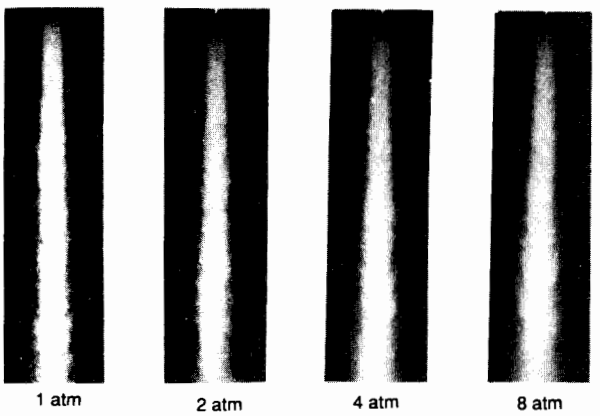

Fig. 2 Flash photographs at various ambient pressures for fully-developed flow.

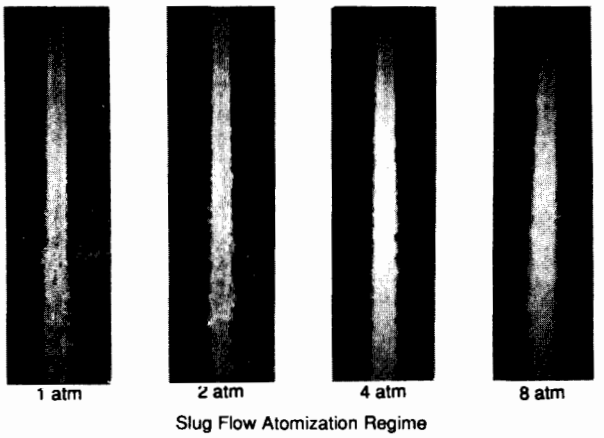

Fig. 3 Flash photographs at various ambient pressures for slug flow.

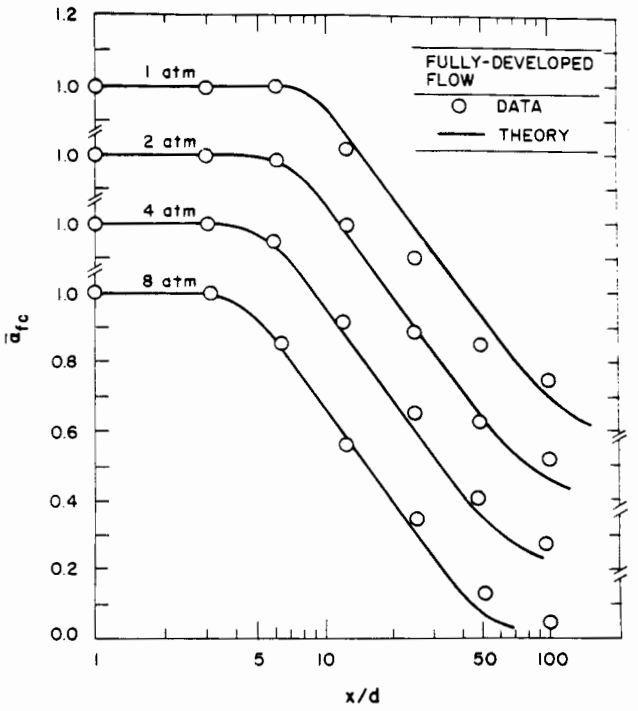

Fig. 4 Time-averaged liquid volume fractions along the axis at various ambient pressures for fully-developed flow.

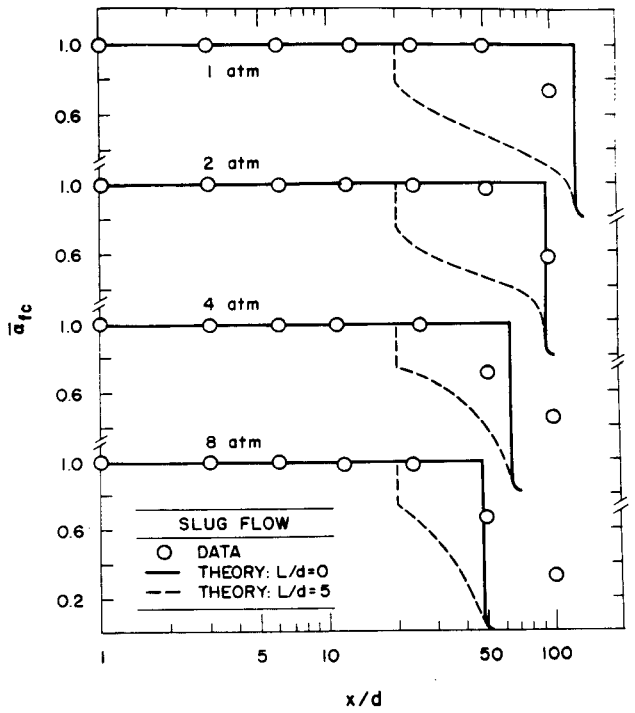

Fig. 5 Time-averaged liquid volume fractions along the axis at various pressures for slug flow.

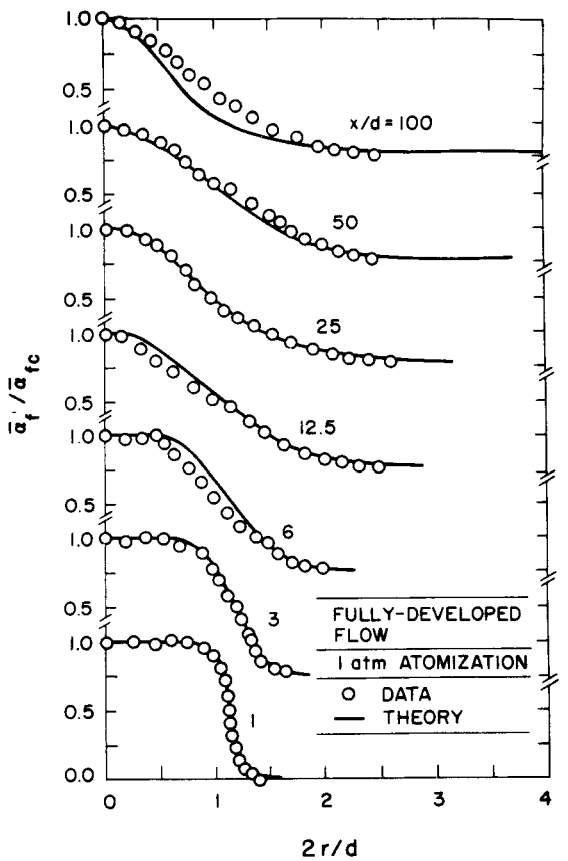

Fig. 6 Radial profiles of mean liquid volume fractions for fully-developed flow at 1 atm.

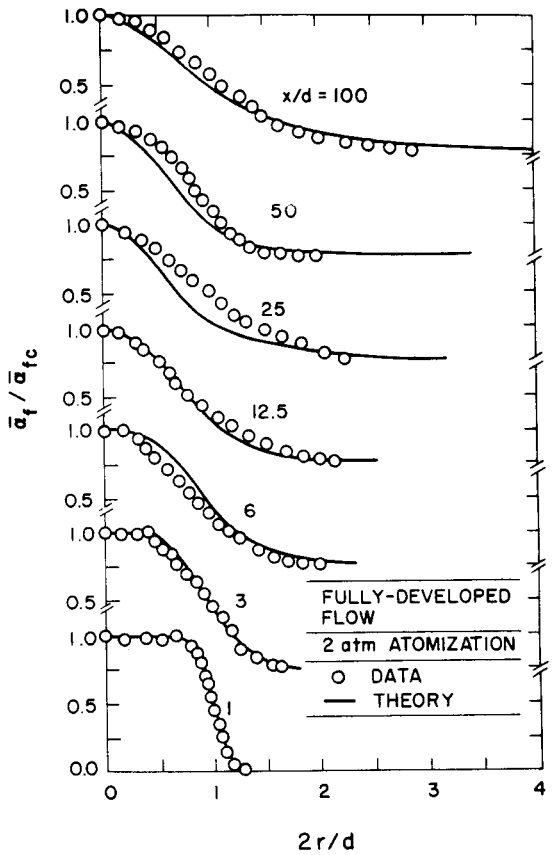

Fig. 7 Radial profiles of mean liquid volume fractions for fully-developed flow at 2 atm.

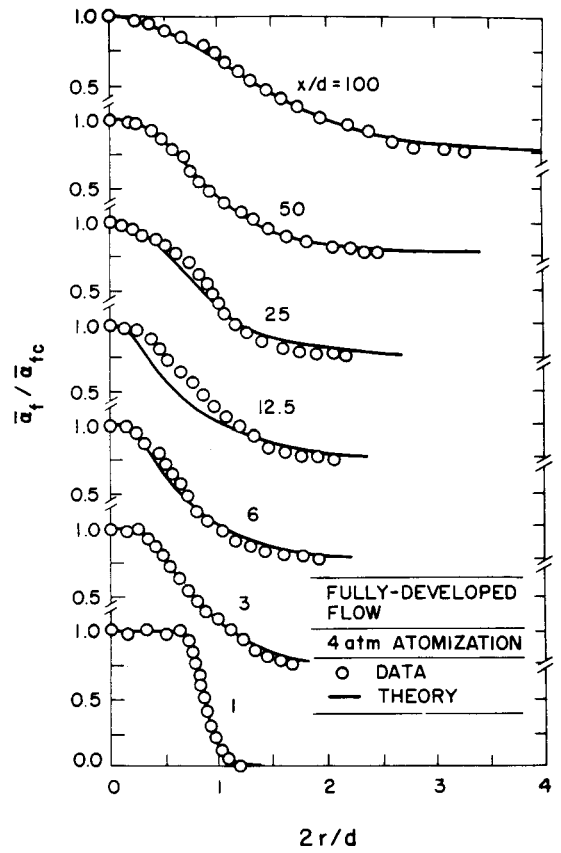

Fig. 8 Radial profiles of mean liquid volume fractions for fully-developed flow at 4 atm.

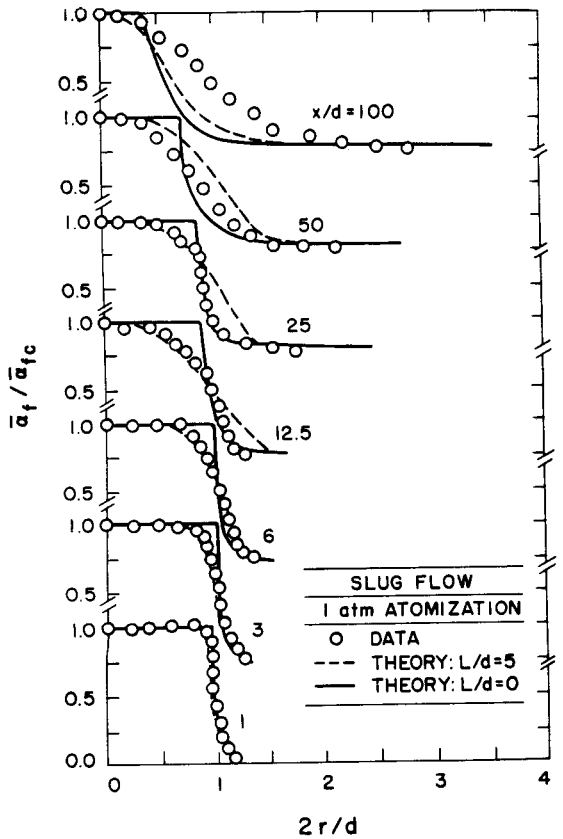

Fig. 9 Radial profiles of mean liquid volume fractions for slug flow at 1 atm.

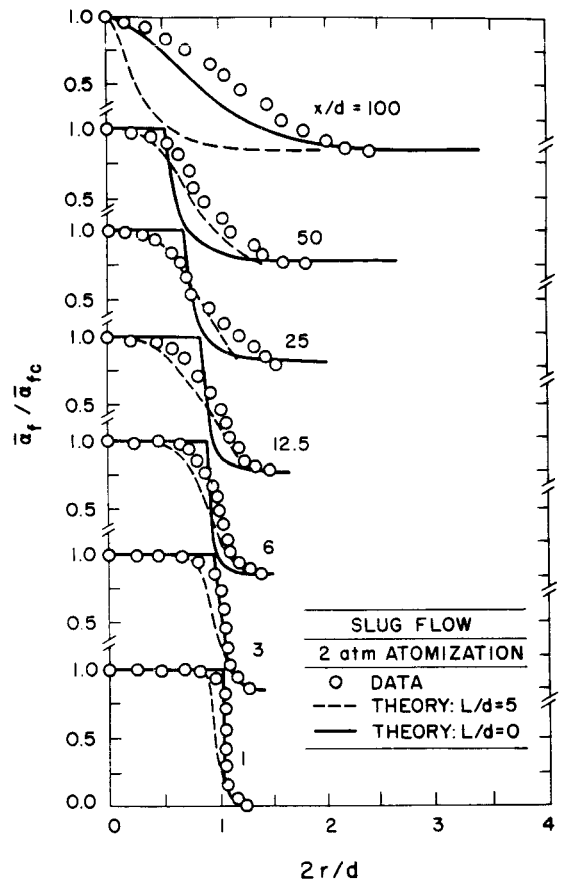

Fig. 10 Radial profiles of mean liquid volume fractions for slug flow at 2 atm.

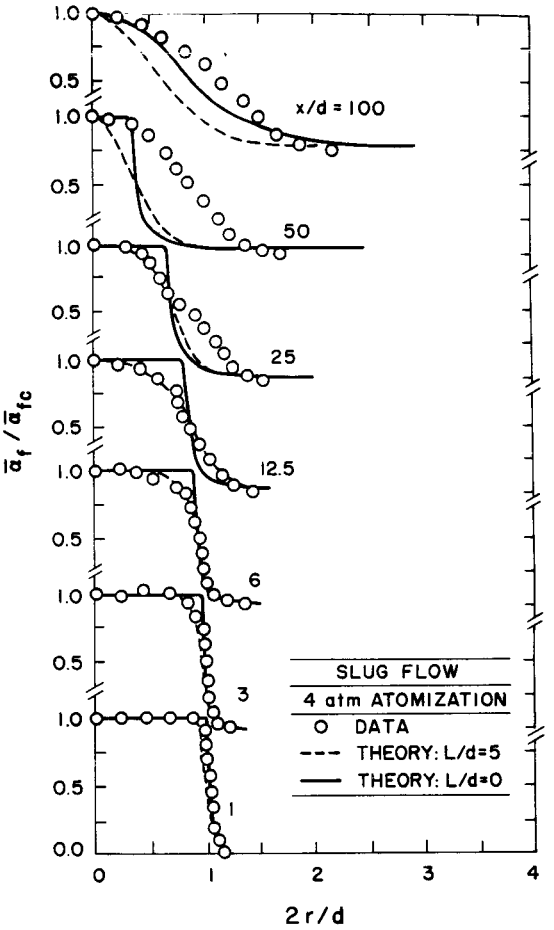

Fig. 11 Radial profiles of mean liquid volume fractions for slug flow at 4 atm.